


Article

Evaluation of an Ozone-Induced Free Radical Solution's Characteristics and Its Efficacy as an Alternative Pest Control Method

Chundu Wu ¹, Peng Tang ¹ , Aineng Cao ², Pengfei Ni ¹, Bo Zhang ^{1,*} and Zhongwei Chang ²

¹ School of the Environment and Safety Engineering, Jiangsu University, Zhenjiang 212013, China; tpsaf1998@163.com (P.T.); npfcjds@163.com (P.N.)

² School of Agricultural Engineering, Jiangsu University, Zhenjiang 212013, China

* Correspondence: tabol@126.com

Abstract: In light of the environmental problems stemming from chemical pesticides, a preparation system for an ozone-induced free radical solution was developed to replace chemical pesticides for disease control. The effective synthesis process parameters for the solution under experimental conditions were determined through a single-factor experiment. The mechanism by which the solution eradicates pathogenic bacteria was investigated using electron microscopy, and a disease prevention and control experiment was conducted. Under slightly acidic conditions, the redox potential of the solution was observed to be high, with an air intake of 0.5 L/min and a liquid intake of 1.45 L/min, while the concentration decayed slowly, with a liquid intake of 0.98 L/min. The solution's destructive effect on the bacteria's internal and external structures intensified with prolonged action time and an increased number of free radicals. A 1.5 mg/L solution and 5% imidacloprid effectively reduced pest levels to grades 3 and 4, respectively. When the pH is 3, with air intake at 0.5 L/min and liquid intake at 0.98 L/min, the ozone-induced free radical solution exhibits strong oxidation and stability. At a concentration of 1.5 mg/L, the solution demonstrates a superior control effect on diseases and can partially replace chemical pesticides, offering a promising alternative for environmentally sustainable disease control.

Keywords: substitute pesticides; ozone; free radical; pest control; insecticide



Citation: Wu, C.; Tang, P.; Cao, A.; Ni, P.; Zhang, B.; Chang, Z. Evaluation of an Ozone-Induced Free Radical Solution's Characteristics and Its Efficacy as an Alternative Pest Control Method. *Appl. Sci.* **2024**, *14*, 3111. <https://doi.org/10.3390/app14073111>

Academic Editor: Franco Mutinelli

Received: 1 March 2024

Revised: 29 March 2024

Accepted: 1 April 2024

Published: 8 April 2024



Copyright: © 2024 by the authors. Licensee MDPI, Basel, Switzerland. This article is an open access article distributed under the terms and conditions of the Creative Commons Attribution (CC BY) license (<https://creativecommons.org/licenses/by/4.0/>).

1. Introduction

China is recognized as the country with the highest production and consumption of pesticides globally [1]. In 2020, pesticide usage in China amounted to 1.31 million tons, constituting 34.5% of the global total [2]. The excessive use of pesticides has resulted in significant pesticide residues in agricultural products. Long-term consumption of agricultural products with pesticide residues may lead to adverse health effects, including chronic poisoning, impairment of the nervous and endocrine systems, and detrimental impacts on children's intellectual development [3,4]. In addition, chemical pesticides enter ecosystems [5] via soil, water, and other pathways, resulting in serious environmental pollution, destabilizing ecological balance, and contributing to a loss of biodiversity [6]. Therefore, reducing environmental pollution from pesticides through the development of environmentally friendly alternatives to traditional chemical pesticides for pest control is of paramount importance.

In recent years, researchers have focused on developing environmentally friendly pesticides as alternatives to traditional ones to mitigate environmental pollution [7,8]. Ozone radical solution is defined as a strong oxidizing solution containing active groups including ozone molecules, hydroxyl groups, and singlet oxygen. In water, gaseous reactive oxygen species (O_2^+ , O , (O^3P) , O_3 , O_2^- , etc.), produced through dielectric barrier discharge, initiate a series of free radical chain reactions following high-pressure gas-liquid mixing,

eventually transforming into a solution rich in liquid free radicals including $\cdot OH$, 1O_2 , $\cdot HO_2^-$, and $\cdot O_2^-$. The solution exhibits several key characteristics: Firstly, it possesses a strong oxidizing property [9]. The $\cdot OH$ radical in the solution possesses a significantly greater oxidizing capability than other chemical oxidants. The reaction's final products are CO_2 , water, and other non-polluting substances. Secondly, it has a broad spectrum [10]. These free radicals initiate and participate in chain reactions, breaking down organic pollutants and attacking a wide array of microorganisms and pests. Thirdly, the free radical reaction rate constants range from 10^6 to 10^9 $L \cdot mol^{-1} \cdot s^{-1}$, enabling rapid eradication of microorganisms and pests [11].

Fan [12] introduced a green reaction device that synthesizes a free radical solution using UV and ozone, demonstrating superior biocidal effectiveness compared to traditional disinfectants. Terao [13] utilized hot water and ozone water to effectively reduce the decay of papaya and achieve control over 50% of the disease. Drogoudi [14] discovered that spraying 1.5 ppm and 3.0 ppm ozone water not only effectively inhibited the occurrence of brown rot in nectarines and plums but also demonstrated no toxic effects on the fruits. Abreu [15] determined that ozone water effectively destroyed the salivary glands of *Rhhipicephalus sanguineus sensu lato* and inhibited pest growth. Although the efficacy of ozone-induced free radical solutions as a substitute for pesticides in controlling agricultural pests and diseases has been widely confirmed, studies on the optimum process parameters for the synthesis of ozone-induced free radical solutions under experimental conditions, identifying the primary free radical types, and evaluating the actual disease control efficacy are limited.

In view of the limitations of existing research, this study develops an efficient preparation system for an ozone-induced free radical solution, aiming to synthesize it as an alternative to traditional chemical pesticides. Initially, single-factor experiments determined the synthesis process parameters for the solution (pH, air intake, and liquid intake). Subsequently, fluorescence and ultraviolet–visible spectrophotometry identified the main components of the solution as a hydroxyl radical ($\cdot OH$), superoxide radical ($\cdot O_2^-$), and singlet oxygen (1O_2), establishing the relationship between free radical and solution concentrations. Lastly, *Bacillus subtilis* and cabbage served as test subjects. The bactericidal efficacy of the ozone-induced free radical solution against *Bacillus subtilis* was evaluated using suspension sterilization tests. Scanning and transmission electron microscopy were used to explore the microscopic mechanisms behind the microbicidal action of the ozone-induced free radical solution. The solution's disease control efficacy was verified through disease control tests. This study's preparation of an ozone radical solution offers a novel approach to developing environmentally friendly pesticides and lays a theoretical foundation for exploring alternatives to traditional chemical pesticides.

2. Materials and Methods

2.1. Materials and Reagents

Terephthalic acid (TA), sodium hydroxide (NaOH), citric acid, nitrotetrazolium chloride blue (NBT), Chemical Reagents Co., Ltd. (Shanghai, China); 1,3-diphenylisobenzofuran (DPBF), Shanghai Aladdin Biochemical Technology Co., Ltd. (Shanghai, China); 5% imidacloprid, Henan Saier Agricultural Technology Co., Ltd. (Zhengzhou, China); *Bacillus subtilis*, No.: CGMCC3.28030, Beijing Biotechnology Co., Ltd. (Beijing, China).

2.2. Instruments and Equipment

Ultraviolet–visible spectrophotometer, Agilent, (Santa Clara, CA, USA); fluorescence spectrophotometer, Australia Varian Co., Ltd. (Belrose, NSW, Australia); pH meter, INESA Scientific Instrument Co., Ltd. (Shanghai, China); electronic balance, Shanghai Jingtian Electronic Instrument Co., Ltd. (Shanghai, China); TRO (total reactive oxidant) concentration detector, B&C Electronics; pipette gun, Eppendorf (Enfield, CT, USA); liquid flowmeter, Yuyao Jintai Instrument Co., Ltd. (Yuyao, China); ORP (oxidation reduction potential) meter, Shenzhen Kedida Electronics Co., Ltd. (Shenzhen, China); gas flowmeter, Duchenne (Cambridge,

MA, USA); gas–liquid mixing pump, Guangzhou Fluid Equipment Co., Ltd. (Guangzhou, China); ozone-induced free radical solution preparation device, self-made; scanning electron microscope and transmission electron microscope, Hitachi, Inc. (Tokyo, Japan).

2.3. Test Sites and Varieties

This experiment took place in the Venlo glass greenhouse at the Key Laboratory of Modern Agricultural Equipment under the auspices of the Ministry of Education at Jiangsu University (Zhenjiang, China). Due to its significant representativeness, short growth cycle, susceptibility to diseases, and accessibility, this study selected Chinese cabbage (rape variety) as the experimental subject. Chinese cabbage was cultivated in PP5 plastic cultivation soft pots with an outer diameter of 120 mm, an inner diameter of 111 mm, a bottom diameter of 85 mm, and a height of 108 mm, using nutrient soil as the culture substrate, whose main components included organic peat, mature coconut bran, and perlite. During the experiment, the vegetables were grown naturally under greenhouse conditions, receiving equal volumes of tap water and nutrient solution every 2–3 days.

2.4. Methods

2.4.1. Preparation of Ozone-Induced Free Radical Solution

Building on the foundational research [16–18], this study employed dielectric barrier discharge (DBD) techniques to synthesize an ozone-induced free radical solution. In Figure 1, the synthesis process of the ozone-induced free radical solution is shown: Air is drawn into the system by a vacuum pump (1), and its pressure is regulated by a pressure regulating valve (3). An integrated molecular sieve (4) filters out other gases from the air to generate pure oxygen and regulates the gas flow rate via a flowmeter (5). Oxygen is then introduced into the DBD device (7). The oxygen molecules are excited and ionized into active gaseous radicals. Gaseous free radicals are mixed with pure water sourced from the large water tank (12) via a gas–liquid mixing pump (10). The release head (13) disperses the mixed solution, facilitating efficient mass transfer and mixing of water with gaseous free radicals, including $\cdot O^{2+}$, O , O_2^- , and O^3P , subsequently recombining to produce a solution enriched with free radicals like $\cdot OH$, $\cdot O_2^-$, and $\cdot HO_3$. The produced free radical solution is stored and circulated in the large water tank (12), with the liquid flow rate regulated by a flowmeter (11). The TRO concentration detector (15) and ORP meter (16) measure the TRO mass concentration and ORP, respectively. A peristaltic pump extracts the test solution from the small water tank (14) via a one-way valve. One-way valves are installed in both the large (12) and small (14) water tanks to allow outward venting. The entire system is sealed to prevent external air from interfering with the experiment.

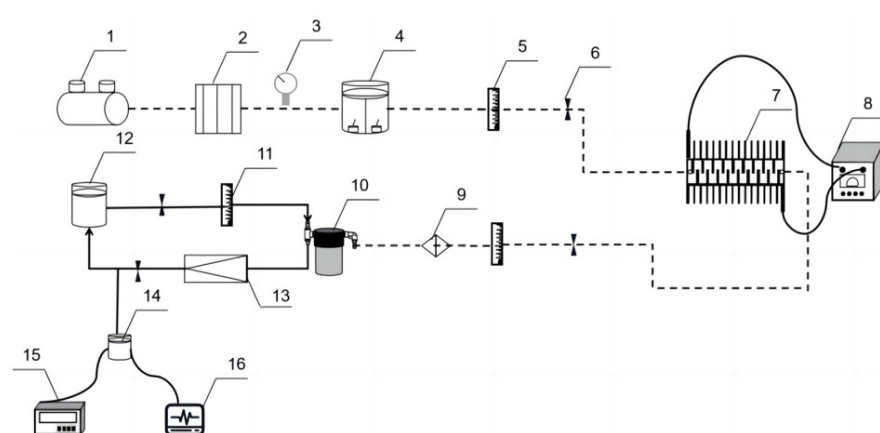


Figure 1. Schematic diagram of ozone-induced free radical solution preparation device. 1: Vacuum pump, 2: copper tube, 3: gas pressure regulating valve, 4: molecular sieve, 5: gas flowmeter, 6: valve, 7: DBD device, 8: high-voltage power supply, 9: one-way valve, 10: gas–liquid mixing pump, 11: liquid flowmeter, 12: large water tank, 13: release head, 14: small water tank, 15: TRO concentration detector, 16: ORP meter.

2.4.2. Analysis of Ozone Radical Solution Oxidation and Stability

During the experiment, the ambient temperature was maintained between 20 °C and 26 °C, and the humidity ranged from 55% to 75%. The device maintained the mass concentration of gaseous free radicals at 110 mg/L, and 5 L of pure water was filled into the large water tank. To investigate the impact of pH on the solution, citric acid/sodium hydroxide was added to the water to adjust the pH to 3.0 ± 0.1 , 5.0 ± 0.1 , 7.0 ± 0.1 , and 9.0 ± 0.1 , with the air and liquid intake rates controlled at 0.1 L/min and 0.8 L/min, respectively. When examining the effect of air intake on the solution, the air intake was adjusted to 0.1 L/min, 0.3 L/min, 0.5 L/min, 0.7 L/min, and 0.9 L/min, with the solution's pH maintained at 7.0 and the liquid intake at 0.8 L/min. Investigating the influence of liquid intake on the solution, the liquid intake was set to 0.8 L/min, 0.98 L/min, 1.2 L/min, and 1.45 L/min, with the solution's pH held at 7.0 and the air intake at 0.1 L/min. For the detection phase, 0.5 L of ozone-induced free radical solution was sampled, with the TRO concentration detector and ORP meter were deployed to record TRO changes over 30 min and ORP variations within the initial 5 min, respectively. This was aimed at investigating the impact of varied pH levels, air intake, and liquid intake on the solution's oxidizability and stability. The effective synthesis parameters of the ozone-induced free radical solution under experimental conditions were determined by a single-factor experiment.

2.4.3. Detection of Free Radical Species in Ozone-Induced Free Radical Solution

- (1) Detection of hydroxyl radical ($\cdot\text{OH}$) [19–22]: Terephthalic acid (TA) undergoes a reaction with hydroxyl radicals, resulting in the formation of 2-hydroxyterephthalic acid (TAOH), with the reaction equation illustrated in Figure 2. A total of 166 mg of TA reagent was dissolved in 100 mL of 1 mol/L NaOH solution (referred to as TA mother liquor), from which 0.1 mL was further diluted to 50 mL to obtain a 10 mmol/L TA solution. A total of 3 mL of the 10 mmol/L TA solution was mixed with 5 mL of the free radical solution, and the emission peak was measured by a fluorescence spectrophotometer at an excitation wavelength of 315 nm and emission of 425 nm.

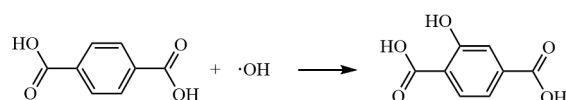


Figure 2. Reaction equation of TA with hydroxyl radical.

- (2) Detection of superoxide radicals ($\cdot\text{O}_2^-$) [23]: Nitroblue tetrazolium chloride (NBT) reacts with superoxide radicals to produce formazan, with the reaction equation depicted in Figure 3. A total of 817.6 mg of NBT was dissolved in 100 mL of pure water to create the mother liquor, from which 0.1 mL was subsequently diluted to 50 mL to achieve a 10 mmol/L NBT solution. A total of 3 mL of the 10 mmol/L NBT solution was mixed with 5 mL of the ozone-induced free radical solution, and the NBT absorption peak at approximately 259 nm was measured using an ultraviolet-visible spectrophotometer. A lower absorption peak compared to the original solution indicates the presence of superoxide radicals.

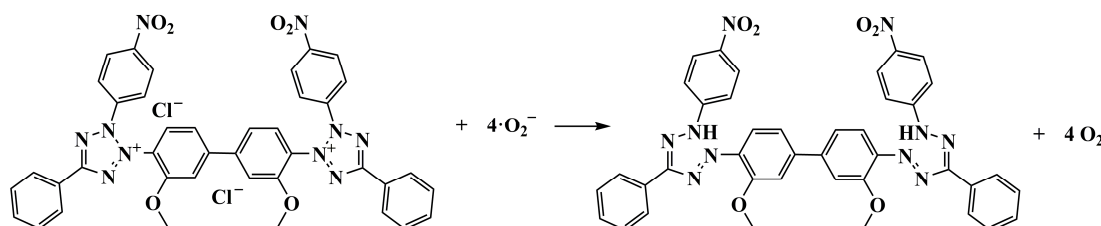


Figure 3. Reaction equation of NBT with superoxide radical.

- (3) Detection of singlet oxygen ($^1\text{O}_2$) [24,25]: 1,3-Diphenylisobenzofuran (DPBF) specifically reacts with singlet oxygen, with the reaction equation presented in Figure 4. A

total of 0.27 g of DPBF was dissolved in 100 mL of pure water to form the mother liquor, from which 0.1 mL was diluted to 50 mL, yielding a 10 mmol/L DPBF solution. A total of 3 mL of the 10 mmol/L DPBF solution was mixed with 5 mL of the ozone-induced free radical solution, and the absorbance at a wavelength of 410 nm was measured using an ultraviolet–visible spectrophotometer, followed by analysis of the absorbance change. A decrease in absorbance indicates the presence of singlet oxygen.

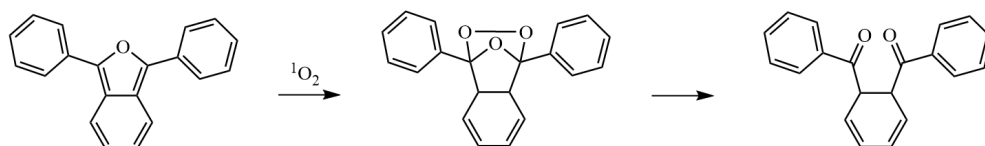


Figure 4. Reaction equation of DPBF with singlet oxygen.

2.4.4. Efficacy Test of Ozone-Induced Free Radical Solution in Controlling Typical Pathogens

Bacillus subtilis served as the experimental subject for investigating the antimicrobial efficacy and mechanisms of the ozone-induced free radical solution via suspension sterilization tests. The concentration of the *Bacillus subtilis* suspension in the experiment ranged from 1×10^5 to 3×10^5 cfu/mL. For enumeration, a gradient group is selected where the colony count in the culture dish is below 300 cfu for accurate counting.

(1) Inhibitory Effect of ozone-induced free radical solution on *Bacillus subtilis*

To assess the inhibitory effect of varying concentrations of the ozone-induced free radical solution, 0.5 mL of bacterial suspension was combined with 4.5 mL of the solution at different concentrations in a test tube, and the mixture was vigorously mixed for 1 min. Six serial dilutions were performed, and 0.1 mL of each dilution was inoculated onto nutrient broth agar Petri dishes. Following a 3-day incubation period, colonies were counted. Exploring the impact of different exposure times on the inhibitory effect, 0.5 mL of bacterial suspension was mixed with 4.5 mL of 0.5 mg/L ozone-induced free radical solution in a test tube, and agitated for durations of 1, 3, 5, and 10 min, respectively, with all subsequent steps mirroring those previously described.

(2) Analysis of the Effect of ozone-induced free radical solution on the Structure of *Bacillus subtilis*

Structural alterations in *Bacillus subtilis* pre- and post-treatment with ozone-induced free radical solution were observed via scanning and transmission electron microscopy, elucidating the solution's microbicidal mechanism [26,27]. The experiment featured a control group (sterile water) and treatment groups with 0.3 mg/L and 0.5 mg/L ozone-induced free radical solution concentrations. Initially, samples were pretreated, with the bacterial suspensions exposed to ozone-induced free radical solution collected via centrifugation. Following a sterile water rinse, samples were fixed in 2.5% glutaraldehyde and refrigerated at 4 °C for a minimum of 2 h. The fixative was removed, and samples were rinsed three times with 0.1 M, pH 7.0 phosphate buffer, 15 min per rinse; thereafter, samples were fixed in 1% osmic acid solution for 1–2 h. Subsequently, osmic acid waste was discarded, and the samples underwent three additional rinses with 0.1 M, pH 7.0 phosphate buffer, each lasting 15 min. Samples underwent dehydration through sequential exposure to ethanol solutions at gradient concentrations (30%, 50%, 70%, 80%, 90%, and 95%) for 15 min, followed by two subsequent treatments with 100% ethanol, each for 20 min.

Scanning electron microscopy (SEM) observation: The pretreated samples underwent treatment with an ethanol and isoamyl acetate mixture (1:1 volume ratio) for 30 min, followed by pure isoamyl acetate treatment for 1 h. This process was succeeded by critical point drying and coating. Images of the treated samples were captured using a scanning electron microscope at an acceleration voltage of 15 kV.

Transmission electron microscopy (TEM) observation: The pretreated samples underwent treatment with pure acetone for 20 min. Subsequently, the sample received treatment

with an embedding agent and acetone mixture (1:1 volume ratio) for 3 h, followed by embedding and overnight heating at 70 °C. Embedded samples were sectioned into 70 to 90 nm slices using an ultra-microtome. Sections were stained with lead citrate and a 50% ethanol-saturated solution of uranium acetate for 5 to 10 min, respectively, before being imaged with a transmission electron microscope at an acceleration voltage of 90 kV.

(3) Pest Control Efficacy in Greengrocery

During the experiment, the Chinese cabbage was subject to natural infection and vulnerable to pests including aphids, planthoppers, whiteflies, leafhoppers, thrips, and leafminers. These pests consume the leaves of Chinese cabbage and extract plant sap, causing symptoms such as yellowing, wilting, and potentially leaf death, posing significant harm. Therefore, this study selected these pests as the focus of control efforts [28,29]. The vegetable pest prevention experiment [30] set up a total of four treatments: A: spraying water; B: spraying 0.5 mg/L ozone-induced free radical solution; C: spraying 1.5 mg/L ozone-induced free radical solution; and D: spraying 5% imidacloprid. The 5% imidacloprid should be diluted 500 times and sprayed once every seven days.

Spray 100 mL of an on-site ozone-induced free radical solution at a distance of 10 cm above the top of the vegetable. Spraying was conducted from 5 pm to 6 pm, with applications on the 1st, 3rd, 5th, and 7th days. Each treatment consisted of three replicate groups, and the results were statistically analyzed after 15 days. Throughout the experiment, vegetables experienced natural infection, with pests categorized into five severity levels. Pests were classified as grade 1 when wormholes occupied over 50% of the total leaf area. Grade 2 pests had wormholes covering 30% to 50% of the leaf area. Grade 3 pests were identified by wormholes spanning 10% to 30% of the leaf area. Pests with wormholes affecting under 10% of the leaf area were designated as grade 4.

2.4.5. Statistical Analysis Methods

In the bacteriostatic experiment, the formula used to calculate the bacterial count is Equation (1), and the calculation formula of the sterilization rate is Equation (2).

$$N(\text{cfu/mL}) = n \times 10^f \times 10 \quad (1)$$

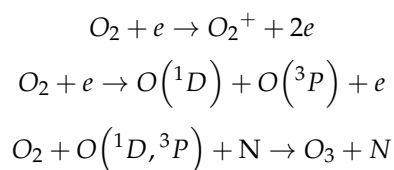
$$C = \frac{N_a - N_b}{N_a} \quad (2)$$

(where N represents the bacterial count, n is the colony count on the culture dish, f denotes the dilution factor, N_a is the bacterial count in the control group, and N_b is the bacterial count in various experimental groups). ORP, TRO, absorbance, wormhole count, and electron microscopy analysis results are directly obtained from instrument readings. All data presented in this study are expressed as averages derived from three trials. Origin software (Version: Origin Pro 2024 SR1) was utilized for data analysis and graphing, while Excel (Version: 2402 Build 16. 0. 17328. 20124) was employed for table creation.

3. Results

3.1. Oxidation and Stability Analysis of Ozone-Induced Free Radical Solution

During the reaction of the synthetic solution, the oxygen molecules are excited and ionized into active gaseous radicals including $\cdot O_2^+$, O , O^3P , O_3 , and $\cdot O^{2-}$ through subsequent excitation reactions:



Among them, N can be O , O_2 , O_3 . Gaseous ozone reacts with hydroxide ions in water to produce hydroxyl radical peroxide (HO_2) and other substances [31]. The reaction process

is as follows: $O_3 + OH^- \rightarrow O_2 + HO_2$. The chemical reactivity of HO_2 is significantly lower than that of hydroxyl radicals ($\cdot OH$), and its reaction with carbon monoxide (CO) may lead to a reduction in both the chemical reactivity and stability of the solution. Consequently, identifying a suitable pH value is crucial for enhancing the efficiency of free radical formation [32]. Both air and liquid intake significantly influence the efficiency of gas–liquid mass transfer. An increase in air intake within a specific range can enhance mass transfer efficiency. A precise amount of liquid ensures full dissolution of gaseous free radicals [33,34]. The total oxidant concentration (TRO) represents the sum of all oxidant concentrations in the solution, accurately reflecting its oxidizability. The redox potential (ORP) reflects the activity of both oxidants and reducing agents in the solution, thereby evaluating its stability [31].

The oxidative potential and stability of the ozone-induced free radical solution are influenced by factors such as pH value [35], air intake [36], and liquid intake [37]. In this study, targeted experiments were conducted to identify the effective parameters for the synthesis process under the experimental conditions.

3.1.1. Effect of pH on Oxidizability and Stability

The ORP value of the ozone radical solution preparation device decreases with an increase in pH value over a period of five minutes in Figure 5. Within the first minute, there is a significant disparity in the ORP values within the solution. The ORP value reaches 1104 mV at a pH of 3, while it stands at 832 mV at a pH of 9. In the subsequent one to five minutes, the ORP value slightly increases, indicating the pH value's impact on the redox potential of the ozone-induced free radical solution, with slightly acidic solutions demonstrating greater oxidative properties.

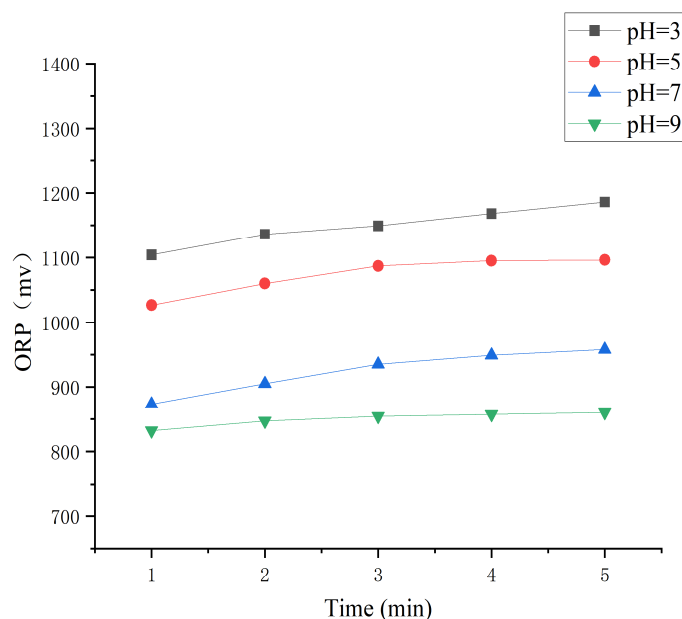


Figure 5. Effect of different pH levels on the oxidation of free radical solutions.

Following a 5 min operation of the ozone-induced free radical solution preparation device, the TRO concentration detector measured the TRO mass concentration's attenuation over a 30 min period. Except for a mass concentration of 5.61 mg/L at pH 5, the initial mass concentrations for other pH values were approximately 10 mg/L. When the pH value ranged from 3 to 9, the decay rates were 48.86%, 38.86%, 89.09%, and 98.81%, respectively. As depicted in Figure 6, Acidic ozone radical solutions demonstrated slower decay rates than alkaline solutions.

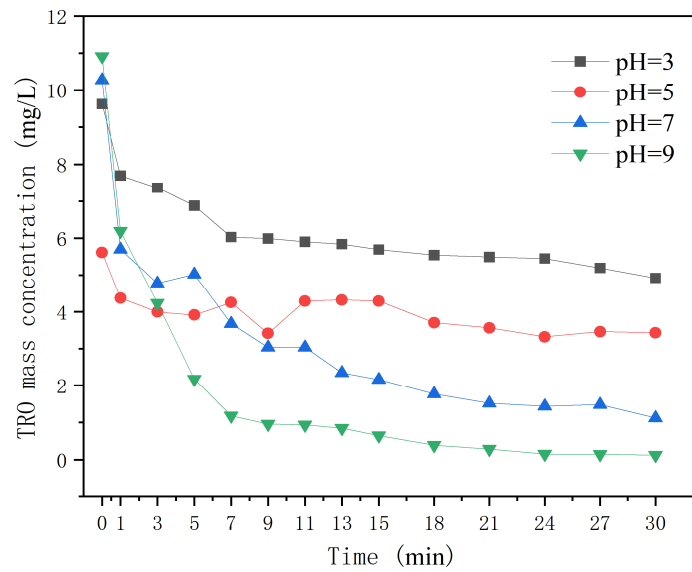


Figure 6. Effects of different pH levels on the stability of free radical solutions.

3.1.2. Effect of Air Intake on Oxidizability and Stability

In Figure 7, with an air intake of 0.5 L/min, the ozone-induced free radical solution exhibits its highest oxidation capacity, achieving an ORP value of 926 mV within 1 min; this represents the most significant increase, being 108 mV higher than when the air intake is 0.1 L/min. The disparity in ORP values across the five pH gradients at 5 min was less pronounced than at 1 min.

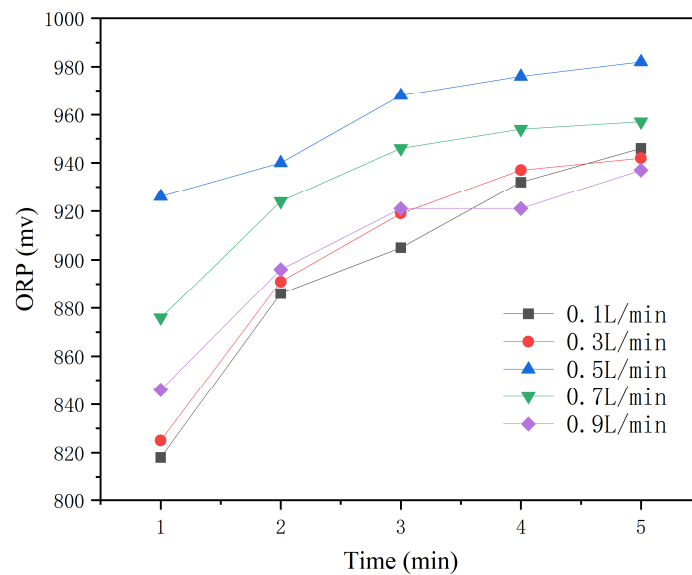


Figure 7. Effect of air intake on the oxidation of free radical solutions.

In Figure 8, the TRO mass concentration across different air intake test groups exhibits a consistent attenuation trend within 30 min, with attenuation efficiency ranging between 75% and 78%. Within the same group, variations during the identical time period remain minimal. Regarding the overall attenuation trend, the TRO mass concentration diminishes more rapidly in the first 5 min and more gradually in the final 15 min.

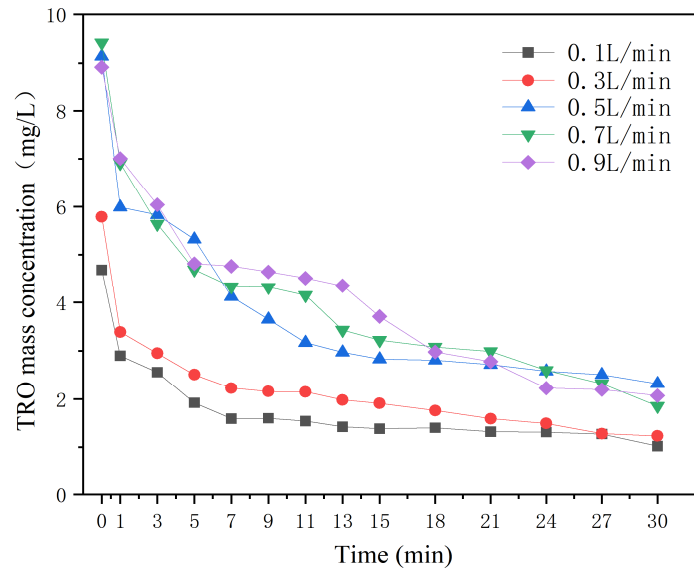


Figure 8. Effect of intake volume on the stability of the free radical solution concentration.

3.1.3. Effect of Liquid Volume on Oxidation and Stability

With a liquid intake of 1.45 L/min, the ORP value tends to be higher. At 5 min, the ORP value shows a 56 mV difference compared to 1 min, indicating a minor variation. When comparing liquid intakes of 0.98 L/min and 1.2 L/min, the ORP difference at 1 min was 45 mV, but it ranged from 1 to 10 mV between 2 and 5 min, indicating a stable overall trend in Figure 9.

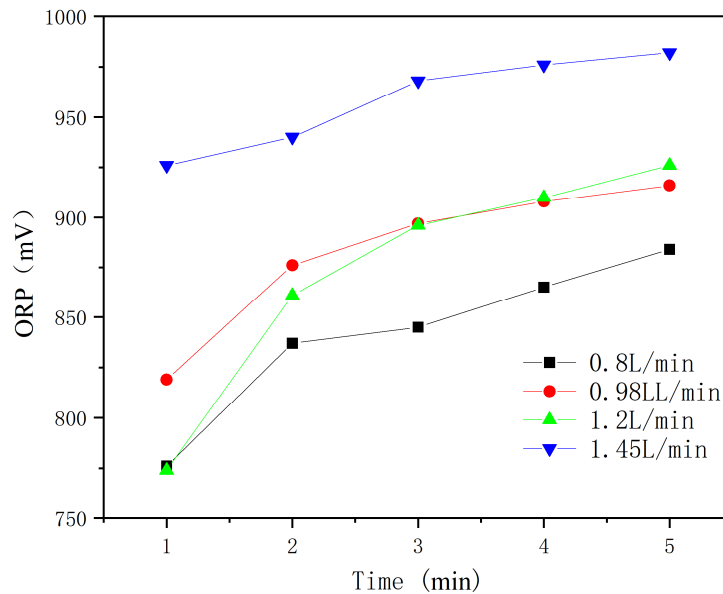


Figure 9. Effect of liquid volume on oxidation of free radical solutions.

It is observed that the initial TRO mass concentration is higher with a liquid intake of 1.2 L/min, decreasing rapidly at 9 min with a decay rate of 63.98% from Figure 10. During the initial 9 min, the mass concentration of TRO may exhibit fluctuations due to on-line monitoring errors at liquid intakes of 0.98 L/min and 1.45 L/min, yet the overall trend remains relatively stable. Beyond 9 min, the attenuation trends across the four inlet volumes stabilize, with attenuation efficiencies of 52.79%, 37.4%, 49.66%, and 50%, respectively. The slowest attenuation occurs in the 0.98 L/min group.

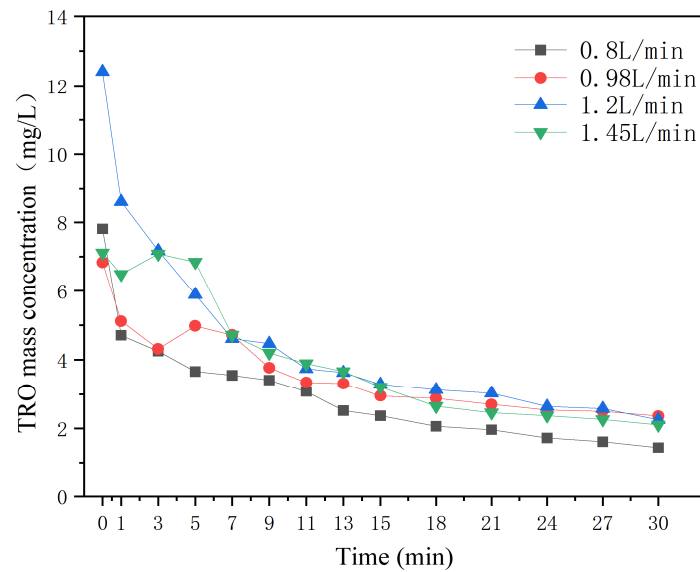
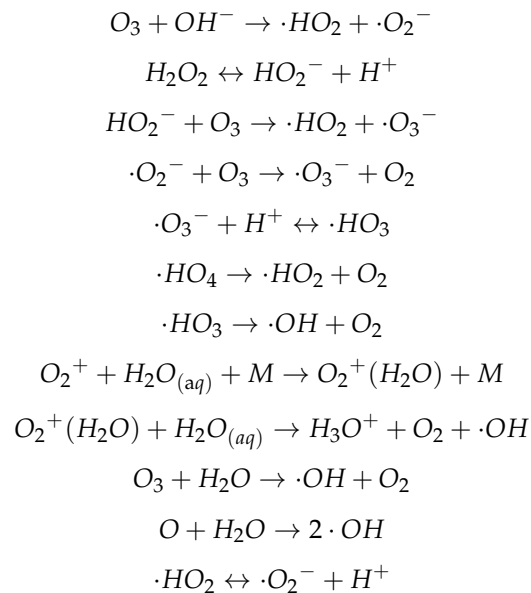


Figure 10. Influence of liquid volume on the stability of the free radical solution concentration.

3.2. Detection of Free Radical Species

In this study, pure water and filtered pure oxygen served as the raw materials for synthesizing the ozone-induced free radical solution. The gas–liquid mixing and sampling processes were completely isolated from the external atmosphere, thereby preventing impurities in water and air (notably, the formation of nitrogen oxides after nitrogen electrolysis) from interfering with the synthesis of the free radical solution.

The interaction between gaseous free radicals and water is illustrated by the following reaction equations:



(M represents an unstable intermediate product). These aforementioned reactions lead to the production of free radicals including $\cdot O_2^+$, $\cdot OH$, O_3 , and $\cdot O_2$ in the solution. Of these, $\cdot OH$, $\cdot O_2^-$ and 1O_2 are pivotal in the oxidative degradation process owing to their high chemical reactivity, significantly influencing the solution's overall performance [38–40]. Ozone in the solution continuously transforms into other free radicals, remaining in an unstable state with a relatively minor impact on the solution's oxidation performance. Consequently, this study primarily investigates the presence of $\cdot OH$, $\cdot O_2^-$, and 1O_2 in the solution.

3.2.1. Hydroxyl Radical

The fluorescence emission peak intensity of TAOH gradually increases and reaches the peak at 470 nm as the solution's mass concentration of TRO increases in Figure 11. At 0.1 mg/L of ozone-induced free radical solution, the fluorescence emission peak reached 248.97. For other mass concentrations, the fluorescence emission peaks were 265.43, 285.55, and 312.52, respectively. The experimental findings confirm that the intensity of the fluorescence emission peak increases with higher solution mass concentrations, indicating the presence of hydroxyl radicals in the solution [41].

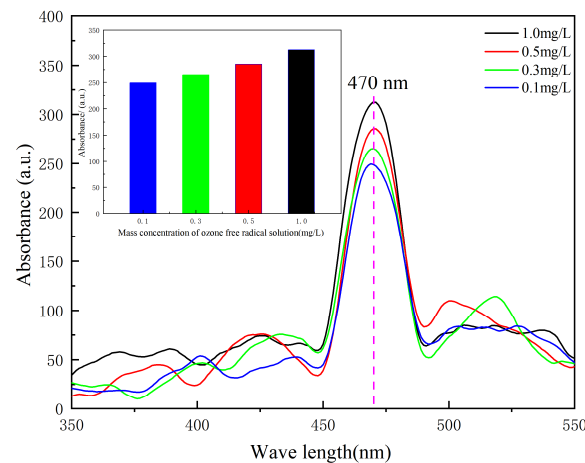


Figure 11. TAOH fluorescence spectrum generated after TA reaction.

3.2.2. Superoxide Radical

The absorption peak at 259 nm significantly decreases as the mass concentration of TRO of the solution increases in Figure 12, following the mixture of NBT solution with varying concentrations of ozone radical solution. At a mass concentration of TRO of 0.1 mg/L, the absorption peak stood at 0.476, decreasing to 0.253 as the concentration rose to 1.0 mg/L—an overall decrease of 46.8%. This suggests the presence of superoxide radicals in the mixed solution, with their content escalating as the solution's concentration increases [42].

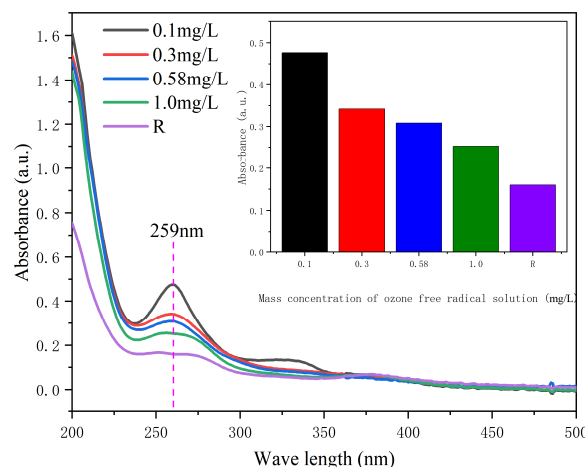


Figure 12. UV absorption spectrum after NBT reaction.

3.2.3. Singlet Oxygen

The spectral absorption peak at 385 nm diminishes as the mass concentration of TRO of the ozone-induced free radical solution increases in Figure 13, following the reaction between the DPBF solution and varying concentrations of ozone-induced free radical solution. At a mass concentration of TRO of 0.1 mg/L for the ozone-induced free radical

solution, the absorption peak of DPBF registered at 0.119. As the mass concentration of TRO of the ozone radical solution escalated to 0.3 mg/L and 0.5 mg/L, the absorption peaks of DPBF were reduced by 19.3% and 35.3%, respectively, suggesting the formation of singlet oxygen during the reaction.

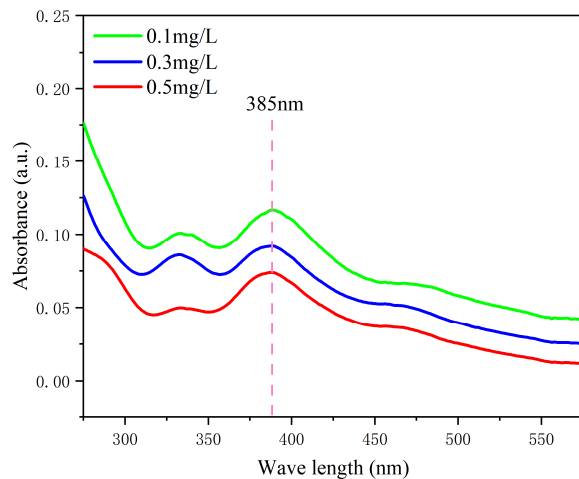


Figure 13. UV absorption spectrum after DPBF reaction.

3.3. Effect of Ozone-Induced Free Radical Solution on Microbial Killing Mechanism and Disease Control

3.3.1. Inhibitory Effect of Ozone-Induced Free Radical Solution on *Bacillus subtilis*

The bactericidal rate of the ozone-induced free radical solution against *Bacillus subtilis* escalates as the mass concentration of TRO increases. At a concentration of 0.3 mg/L, the sterilization rate stood at 51.53%, rising to 87.63% at 0.5 mg/L, and exceeding 99.9% at 1.2 mg/L. Table 1 demonstrates the sterilization rate is directly proportional to the number of free radicals interacting with the bacterial suspension.

Table 1. The bactericidal effect of the free radical solution at different concentrations.

Solution Concentration (mg/L)	Mean Number of Colonies (cfu/mL)	
	<i>Bacillus subtilis</i>	Germicidal Ratio (%)
Control group	2.95×10^5	0
0.3	1.43×10^5	51.53
0.5	3.65×10^4	87.63
0.8	1.8×10^4	93.9
1.2	15	99.99

The sterilization rate of an ozone-induced free radical solution on *Bacillus subtilis* reached 85.10% at 1 min and 97.76% at 10 min, with the growth rate of the sterilization rate decelerating after 5 min. Generally, Table 2 demonstrated that a longer exposure time results in a more effective bactericidal outcome.

Table 2. Effect of treatment time on sterilization by free radical solution.

Treatment Time (min)	Mean Number of Colonies (cfu/mL)	
	<i>Bacillus subtilis</i>	Germicidal Ratio (%)
Control group	2.45×10^4	0
1	3.65×10^4	85.1
3	2.2×10^4	91.02
5	1.95×10^4	92.04
10	5.5×10^3	97.76

3.3.2. Analysis of the Effect of the Ozone-Induced Free Radical Solution on the Structure of *Bacillus subtilis*

The impact of the solution on the external structure of *Bacillus subtilis* was assessed using scanning electron microscopy. Figure 14a presents an electron microscope image prior to solution treatment, depicting the bacteria as straight, rod-shaped, with blunt ends, and uniformly sized. Figure 14b displays the electron microscope image following treatment with a 0.3 mg/L solution, where the cells' external structure exhibits wrinkles and depressions, and the cells appear shrunken without rupture—evidence of the reaction between the ozone-induced free radical solution and the bacteria. Figure 14c shows the electron microscope image post-treatment with a 0.5 mg/L solution, revealing significant cracks, slimes, and pits on the bacterial surface, signifying that a higher mass concentration of TRO of the ozone-induced free radical solution exacerbates cell structure damage.

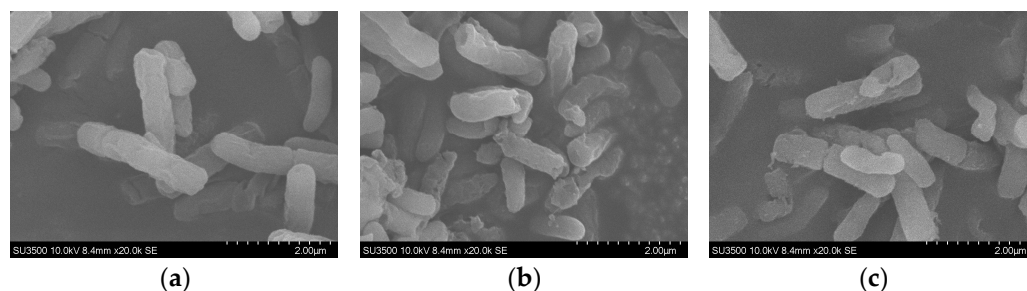


Figure 14. Scanning electron micrograph of *Bacillus subtilis*. (a) Electron microscopy before treatment; (b) electron microscopy after 0.3 mg/L treatment; (c) electron microscopy after 0.5 mg/L treatment.

Damage to the internal structure of *Bacillus subtilis* caused by the solution was evaluated using transmission electron microscopy. Figure 15a depicts the transmission electron microscopy image of the bacteria prior to the solution treatment, showcasing clear visibility of the cell wall and membrane, presence of the periplasmic space, uniform cytoplasm, and visible free organelles. The cell cross-section length measured 560.93 nm (with a scale of 200 nm, applicable to subsequent descriptions). Figure 15b presents the transmission electron microscopy image after treatment with a 0.3 mg/L solution, where the periplasmic space vanished, the distinction between cell wall and membrane blurred, the cytoplasm appeared abnormal, and the cell cross-section length reduced to 548.97 nm. Figure 15c illustrates the transmission electron microscopy image post-0.5 mg/L solution treatment, revealing a thinner cell wall, emergence of air chambers and gaps between the cell walls, and a cell section length of 508.58 nm. In summary, the ozone-induced free radical solution significantly affected both the internal and external structures of the bacteria, with the extent of damage exhibiting a positive correlation with the solution's mass concentration.

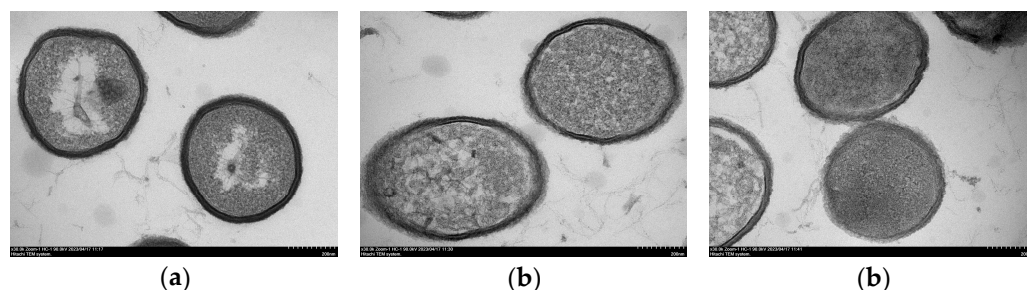






Figure 15. Transmission electron micrograph of *Bacillus subtilis*. (a) Electron microscopy before treatment; (b) electron microscopy after 0.3 mg/L treatment; (c) electron microscopy after 0.5 mg/L treatment.

3.3.3. Pest Control Efficacy in Greengrocery

Observations from the figure (in Table 3) indicate that some leaves appear yellowish, a condition potentially attributable to the soil and growth environment.

Table 3. Effect on disease and insect pest control in Chinese Cabbage.

Treatment Group	Description of the Situation	Control Effect Diagram
(A)	<p>Pest grade: Level 1</p> <p>Description: This group served as the control group, with treatments limited to water spraying. Each Chinese cabbage leaf exhibited 26 wormholes on its surface. The prevalence of wormholes was significant, and the extent of leaf area consumed was considerable, indicating a severe infestation.</p>	
(B)	<p>Pest grade: Level 2</p> <p>Description: A 0.5 mg/L ozone-induced free radical solution was applied to this group. The leaf surface of Chinese cabbage in this group exhibited fewer wormholes compared to control group A, totaling 14. While some damage to the leaf surface was observed, it was markedly less severe than in the control group, indicating a degree of pest control.</p>	
(C)	<p>Pest grade: Level 3</p> <p>Description: The group received a 1.5 mg/L ozone-induced free radical solution spray. The figure illustrates a reduction in the number of wormholes on the surface of Chinese cabbage leaves, totaling 9. This suggests that a high concentration of ozone-induced free radical solution effectively inhibits the disease.</p>	
(D)	<p>Pest grade: Level 4</p> <p>Description: This group was treated with 5% imidacloprid for disease control. The leaves exhibited 6 wormholes, each with a small area.</p>	

4. Discussion

4.1. Oxidation and Stability Analysis of Ozone-Induced Free Radical Solution

Under slightly acidic conditions (pH 3 to 5), the ozone radical solution exhibits slow mass concentration decay and potent oxidation capabilities. This observation can be attributed to slightly acidic conditions where the presence of H^+ stabilizes the free radical reaction intermediates, enhancing the production of free radicals. Consequently, this increases both the concentration and the stability of free radicals in the solution [43], indicating that slightly acidic conditions favor free radical solution synthesis.

Gas free radical intake between 0.5 and 0.7 L/min shows comparable mass concentration stability, with stronger oxidation observed at 0.5 L/min. At a liquid volume of 1.45 L/min, the ozone-induced free radical solution exhibits a high redox potential value, while a slower decay rate is observed at 0.98 L/min. Higher air intake can bring more gaseous free radicals to the reaction, thereby increasing the number of liquid free radicals in the solution, and ultimately leading to improved oxidation performance. By changing the concentration of free radicals in the solution, the amount of liquid inlet affects the

reaction equilibrium and rate of gas–liquid mixing, and changes the oxidation and stability of the solution. Previous studies have shown that [34], when the gas and liquid flow rate increases, the resistance of the liquid applied to the gas will increase, bringing more ozone gas molecules. This will cause the ozone bubbles to break into smaller bubbles and increase the gas–liquid contact area. At the same time, the continuous folding and stretching of bubbles will lead to higher shear rates, forming a thinner liquid film and improving gas–liquid mass transfer efficiency. However, if the gas–liquid flow rate is too high, the gas–liquid contact residence time will be shortened and the efficiency of gas–liquid mass transfer will be reduced. Therefore, it is necessary to find a suitable air intake and liquid intake to synthesize an ozone-induced free radical solution more efficiently. These parameters can be used as a preliminary attempt to synthesize more effective process parameters for an ozone-induced free radical solution.

4.2. Detection of Free Radical Species

The determination of free radical types revealed the presence of hydroxyl radicals, superoxide radicals, and singlet oxygen in the solution. The concentrations of hydroxyl and superoxide radicals generated in the ozone-induced free radical solution are positively correlated with the solution's mass concentration. Simultaneously, the concentration of singlet oxygen increases with the solution's mass concentration, evidenced by a rise in DPBF consumption from 0.1 mg/L to 0.5 mg/L and a 35.3% reduction in the absorption peak, confirming the presence and consumption of singlet oxygen. This phenomenon occurs because TRO encompasses all residual oxidizing agents (typically comprising free radicals and other non-radical oxidants), given that free radicals are highly reactive entities possessing unpaired electrons and constitute the primary source of the strong oxidizing capability in free radical solutions. Consequently, an increase in the solution's TRO mass concentration not only augments the total oxidation capacity but also signifies a rise in the concentration of free radicals.

4.3. Effect of Ozone-Induced Free Radical Solution on Microbial Killing Mechanism and Disease Control

As the concentration of the ozone-induced free radical solution increases, so does the quantity of the free radicals, leading to a higher sterilization rate. Under consistent experimental conditions, an extension in treatment time results in an upward trend in bactericidal efficacy. Increasing the mass concentration of the ozone-induced free radical solution intensifies damage to the cell structure of *Bacillus subtilis*, manifesting as cracks, voids, depressions, thinning and rupture of the cell wall, and the formation of gas chambers within the cells. The observed outcomes stem from the high oxidative reactivity of free radicals, capable of interacting with various cellular molecules, with these outcomes including lipid peroxidation, protein damage, and nucleic acid oxidation, thereby causing damage to bacterial cell structures and functional loss. Furthermore, within a specific concentration range, as the TRO mass concentration increases and the exposure time extends, the quantity of free radicals capable of disrupting microbial cell structures rises, consequently enhancing the killing efficacy and extent of structural damage to *Bacillus subtilis*. Oxidative stress induced by these free radicals frequently triggers oxidative reactions in harmful microorganisms, compromising their cell membrane integrity and energy metabolism enzymes, leading to structural and physiological dysfunction in bacteria and ultimately causing their physiological activities to cease [44]. Additionally, these findings elucidate the inhibitory impacts of the ozone-induced free radical solution on harmful microorganisms and its underlying microbicidal mechanism.

The 1.5 mg/L ozone-induced free radical solution and 5% imidacloprid demonstrated effective control over pests in leafy greens, reducing pest severity from grade 1 to grades 3 and 4, respectively, thereby offering protection to Chinese cabbage. The application of ozone-induced free radical solution can damage certain physiological organs of pests, leading to disruptions in their physiological activities. This ultimately results in the ef-

fective inhibition of pest populations [15]. Xu applied ozone water for *Plutella xylostella* management, achieving a control efficacy of 76.4% and a larvae reduction rate of 59.3% [45]. Collectively, these findings underscore the potential of utilizing ozone-induced free radical solutions as alternatives to conventional chemical pesticides.

Research on the ozone-induced free radical solution indicates that plants' physiological responses to this solution vary according to crop species and external environmental factors. An excessively high concentration of the ozone-induced free radical solution can inhibit rice and other crops. The control effect of the ozone-induced free radical solution varies across different plant diseases. Recent studies have demonstrated that the ozone-induced free radical solution is effective in controlling cucumber powdery mildew, tomato nematodes, and other diseases [46]. Future research should further investigate the effects of varying crops, growth cycles, spray volumes, methods, timing, and environmental parameters on crop growth, disease control, fruit quality, and yield after ozone-induced free radical solution application. Additionally, expansion to include disease prevention in outdoor vegetables, fruits, plants, and flowers is warranted [47,48].

5. Conclusions

In this study, an ozone-induced free radical solution was synthesized using the dielectric barrier discharge (DBD) method. The effective synthesis parameters for an ozone-induced free radical solution under experimental conditions were identified through a single-factor experiment, including a pH of 3, air intake of 0.5 L/min, and liquid intake of 0.98 L/min. The presence of a hydroxyl radical ($\cdot OH$), superoxide radical ($\cdot O_2^-$), and singlet oxygen (1O_2) in the solution was confirmed via fluorescence and ultraviolet–visible spectrophotometry, elucidating the positive correlation between free radical concentration and the solution's TRO mass concentration. Suspension sterilization tests and electron microscopy analysis revealed that the ozone-induced free radical solution induced damage to the cell wall of *Bacillus subtilis*, resulting in cytoplasm leakage. Ultimately, the solution exhibited a potent bactericidal effect against *Bacillus subtilis*, with a peak killing rate of 99.99%. The control experiment on cabbage diseases confirmed the solution's efficacy in reducing disease severity from grade 1 to grade 3. This introduces a groundbreaking approach for replacing conventional chemical pesticides in pest management, potentially mitigating environmental pollution.

Author Contributions: Conceptualization, P.T. and C.W.; methodology, A.C.; software, P.T. and A.C.; validation, Z.C., B.Z. and P.T.; formal analysis, P.T.; investigation, P.T. and P.N.; resources, C.W.; data curation, P.T.; writing—original draft preparation, P.T.; writing—review and editing, P.N. and P.T.; visualization, P.T.; supervision, B.Z.; project administration, C.W. and B.Z.; funding acquisition, C.W. All authors have read and agreed to the published version of the manuscript.

Funding: This work was supported by the Jiangsu Province Science and Technology Support Plan (BE2022338).

Institutional Review Board Statement: Not applicable.

Informed Consent Statement: Not applicable.

Data Availability Statement: The data presented in this study are available on request from the corresponding author due to the research data being intended for the project's conclusion within the research group; therefore, to access the data, an application must be submitted to the head of the research group for approval.

Conflicts of Interest: The authors declare no conflicts of interest.

References

1. Jing, Q.; Liu, J.; Chen, A.; Chen, C.; Liu, J. The Spatial–Temporal Chemical Footprint of Pesticides in China from 1999 to 2018. *Environ. Sci. Pollut. Res.* **2022**, *29*, 75539–75549. [[CrossRef](#)] [[PubMed](#)]
2. Li, Z.; Li, C.; Wang, L. Have Pesticides and Fertilizers Improved Agricultural Development? The Threshold Effect Based on China's Agricultural Film Usage. *Appl. Sci.* **2023**, *14*, 6. [[CrossRef](#)]

3. Arab, A.; Mostafalou, S. Neurotoxicity of Pesticides in the Context of CNS Chronic Diseases. *Int. J. Environ. Health Res.* **2022**, *32*, 2718–2755. [[CrossRef](#)]
4. Pascale, A.; Laborde, A. Impact of Pesticide Exposure in Childhood. *Rev. Environ. Health* **2020**, *35*, 221–227. [[CrossRef](#)]
5. Mit, N.; Cherednichenko, O.; Mussayeva, A.; Khamdiyeva, O.; Amirgalieva, A.; Begmanova, M.; Tolebaeva, A.; Koishekenova, G.; Zaypanova, S.; Pilyugina, A.; et al. Ecological Risk Assessment and Long-Term Environmental Pollution Caused by Obsolete Undisposed Organochlorine Pesticides. *J. Environ. Sci. Health Part B* **2021**, *56*, 490–502. [[CrossRef](#)] [[PubMed](#)]
6. Ojija, F.; Bacaro, G. Characterization of Insect–Pollinator Biodiversity in Agrochemical-Contaminated Agricultural Habitats. *Diversity* **2024**, *16*, 33. [[CrossRef](#)]
7. Romeo-Oliván, A.; Pagès, M.; Breton, C.; Lagarde, F.; Cros, H.; Yobrégat, O.; Violleau, F.; Jacques, A. Ozone Dissolved in Water: An Innovative Tool for the Production of Young Plants in Grapevine Nurseries? *Ozone Sci. Eng.* **2022**, *44*, 521–535. [[CrossRef](#)]
8. Da Costa, A.R.; Faroni, L.R.D.; Salomão, L.C.C.; Cecon, P.R.; De Alencar, E.R. Use of Ozonized Water to Control Anthracnose in Papaya and Its Effect on the Quality of the Fruits. *Ozone Sci. Eng.* **2021**, *43*, 384–393. [[CrossRef](#)]
9. Zou, L.; Wang, Y.; Huang, C.; Li, B.; Lyu, J.; Wang, S.; Lu, H.; Li, J. Meta-Cresol Degradation by Persulfate through UV/O₃ Synergistic Activation: Contribution of Free Radicals and Degradation Pathway. *Sci. Total Environ.* **2021**, *754*, 142219. [[CrossRef](#)]
10. Cheng, G.; Li, Z.; Sun, L.; Li, Y.; Fu, J. Application of Microwave/Electrodeless Discharge Ultraviolet/Ozone Sterilization Technology in Water Reclamation. *Process Saf. Environ. Prot.* **2020**, *138*, 148–156. [[CrossRef](#)]
11. Hardison, D.R.; Cooper, W.J.; Mezyk, S.P.; Bartels, D.M. The Free Radical Chemistry of Tert-Butyl Formate: Rate Constants for Hydroxyl Radical, Hydrated Electron and Hydrogen Atom Reaction in Aqueous Solution. *Radiat. Phys. Chem.* **2002**, *65*, 309–315. [[CrossRef](#)]
12. Fan, X.; Song, Y. Advanced Oxidation Process as a Postharvest Decontamination Technology to Improve Microbial Safety of Fresh Produce. *J. Agric. Food Chem.* **2020**, *68*, 12916–12926. [[CrossRef](#)]
13. Terao, D.; De Lima Nechet, K.; Shiraiishi Frighetto, R.T.; Cerqueira Sasaki, F.F. Ozonated Water Combined with Heat Treatment to Control the Stem-End Rot of Papaya. *Sci. Hortic.* **2019**, *257*, 108722. [[CrossRef](#)]
14. Drogoudi, P.; Pantelidis, G.; Thomidis, T. Impact of Ozonated Water on Brown Rot Development and Storage Potential of Nectarine and Plum. *Ozone Sci. Eng.* **2023**, *45*, 410–418. [[CrossRef](#)]
15. Abreu, M.R.; Delalibera, I.; Pereira, N.R.C.; Camargo-Mathias, M.I. Morphophysiological Analysis of the Salivary Glands of *Rhipicephalus sanguineus* Sensu Lato (Acari: Ixodidae) Exposed to Ozonated Water: A Control Strategy. *Med. Vet. Entomol.* **2021**, *35*, 88–96. [[CrossRef](#)] [[PubMed](#)]
16. Chebbah, A.; Hadjeri, S.; Nemmich, S.; Nassour, K.; Zouzou, N.; Tilmatine, A. Development and Experimental Analysis of a New “Serpentine-Shape” Surface-DBD Ozone Generator—Comparison with a Cylindrical Volume-DBD Ozone Generator. *Ozone Sci. Eng.* **2017**, *39*, 209–216. [[CrossRef](#)]
17. Park, J.; Park, J.; Lee, J.; Jeong, B. Space Sterilization Effect through High-Density Plasma Ozone Using DBD Device. *J. Electr. Eng. Technol.* **2022**, *17*, 2771–2778. [[CrossRef](#)]
18. Jodzis, S.; Barczyński, T. Ozone Synthesis and Decomposition in Oxygen-Fed Pulsed DBD System: Effect of Ozone Concentration, Power Density, and Residence Time. *Ozone Sci. Eng.* **2019**, *41*, 69–79. [[CrossRef](#)]
19. Masek, A.; Chrzescijanska, E.; Latos-Brozio, M.; Zaborski, M. Characteristics of Juglone (5-Hydroxy-1,4-Naphthoquinone) Using Voltammetry and Spectrophotometric Methods. *Food Che.* **2019**, *301*, 125279. [[CrossRef](#)]
20. Yu, Y.X.; Bai, M.D.; Yang, X.T.; Ji, Z.X.; Li, J.; Yao, L. Hydroxyl radical degradation of norfloxacin in high algae drinking water system. *China’s Environ. Sci.* **2018**, *38*, 4545–4550. [[CrossRef](#)]
21. Khan, Z.U.H.; Gul, N.S.; Sabahat, S.; Sun, J.; Tahir, K.; Shah, N.S.; Muhammad, N.; Rahim, A.; Imran, M.; Iqbal, J.; et al. Removal of Organic Pollutants through Hydroxyl Radical-Based Advanced Oxidation Processes. *Ecotoxicol. Environ. Saf.* **2023**, *267*, 115564. [[CrossRef](#)] [[PubMed](#)]
22. Zhao, Y.; Shi, H.; Hu, X.; Liu, E.; Fan, J. Fabricating CsPbX₃/CN Heterostructures with Enhanced Photocatalytic Activity for Penicillins 6-APA Degradation. *Chem. Eng. J.* **2020**, *381*, 122692. [[CrossRef](#)]
23. Zhao, Y.; Liang, X.; Shi, H.; Wang, Y.; Ren, Y.; Liu, E.; Zhang, X.; Fan, J.; Hu, X. Photocatalytic Activity Enhanced by Synergistic Effects of Nano-Silver and ZnSe Quantum Dots Co-Loaded with Bulk g-C₃N₄ for Ceftriaxone Sodium Degradation in Aquatic Environment. *Chem. Eng. J.* **2018**, *353*, 56–68. [[CrossRef](#)]
24. Entradas, T.; Waldron, S.; Volk, M. The Detection Sensitivity of Commonly Used Singlet Oxygen Probes in Aqueous Environments. *J. Photochem. Photobiol. B Biol.* **2020**, *204*, 111787. [[CrossRef](#)] [[PubMed](#)]
25. Tian, N.; Zhang, Y.; Li, X.; Xiao, K.; Du, X.; Dong, F.; Waterhouse, G.I.N.; Zhang, T.; Huang, H. Precursor-Reforming Protocol to 3D Mesoporous g-C₃N₄ Established by Ultrathin Self-Doped Nanosheets for Superior Hydrogen Evolution. *Nano Energy* **2017**, *38*, 72–81. [[CrossRef](#)]
26. Pang, B.; Huang, L.; Teng, J.; Zhang, J.; Xia, N.; Wei, B. Effect of Pile Fermentation on the Cells of Chinese Liupao Tea: The First Record of Cell Wall of Liupao Tea on Transmission Electron Microscope. *Food Chem.* **2021**, *361*, 130034. [[CrossRef](#)] [[PubMed](#)]
27. Hickey, W.J.; Shetty, A.R.; Massey, R.J.; Toso, D.B.; Austin, J. Three-dimensional Bright-field Scanning Transmission Electron Microscopy Elucidate Novel Nanostructure in Microbial Biofilms. *J. Microsc.* **2017**, *265*, 3–10. [[CrossRef](#)] [[PubMed](#)]
28. Malinga, L.N.; Laing, M.D. Efficacy of Three Biopesticides against Cotton Pests under Field Conditions in South Africa. *Crop Prot.* **2021**, *145*, 105578. [[CrossRef](#)]

29. Kamakshi, N.; Neelima, S.; Venkataramanamma, K.; Kalyani, D.L. Efficacy of Insecticides Against Thrips, Leafhoppers and Whiteflies in Sunflower. *Indian J. Entomol.* **2021**, *83*, 595–597. [[CrossRef](#)]
30. Egel, D.S.; Hoagland, L.; Davis, J.; Marchino, C.; Bloomquist, M. Efficacy of Organic Disease Control Products on Common Foliar Diseases of Tomato in Field and Greenhouse Trials. *Crop Prot.* **2019**, *122*, 90–97. [[CrossRef](#)]
31. Buchan, K.A.H.; Martin-Robichaud, D.J.; Benfey, T.J. Measurement of Dissolved Ozone in Sea Water: A Comparison of Methods. *Aquac. Eng.* **2005**, *33*, 225–231. [[CrossRef](#)]
32. Nghi, N.H.; Cuong, L.C.; Dieu, T.V.; Oanh, D.T.Y. Study of Water Disinfection by Analyzing the Ozone Decomposition Process. *Vietnam J. Chem.* **2018**, *56*, 591–595. [[CrossRef](#)]
33. Liu, T.; Zhang, B.; Li, W.; Li, B.; Han, Z.; Zhang, Y.; Ding, A.; Wang, S.; Ma, J.; He, X. The Catalytic Oxidation Process of Atrazine by Ozone Microbubbles: Bubble Formation, Ozone Mass Transfer and Hydroxyl Radical Generation. *Chemosphere* **2023**, *325*, 138361. [[CrossRef](#)] [[PubMed](#)]
34. Pituco, M.M.; Marrocos, P.H.; Santos, R.J.; Dias, M.M.; Lopes, J.C.B.; Moreira, F.C.; Vilar, V.J.P. NETmix Technology as Ozone Gas Injection System: Assessment of the Gas-Liquid Mass Transfer. *Chem. Eng. Process. Process Intensif.* **2023**, *194*, 109566. [[CrossRef](#)]
35. De Rezende, A.J.; De Alencar, E.R.; Ferreira, M.D.A.; Ferreira, W.F.D.S. Control of *Listeria monocytogenes* in Refrigerated Ozonated Water. *Ozone Sci. Eng.* **2022**, *44*, 281–290. [[CrossRef](#)]
36. Wang, B.; Xiong, X.; Shui, Y.; Huang, Z.; Tian, K. A Systematic Study of Enhanced Ozone Mass Transfer for Ultrasonic-Assisted PTFE Hollow Fiber Membrane Aeration Process. *Chem. Eng. J.* **2019**, *357*, 678–688. [[CrossRef](#)]
37. Prada-Vásquez, M.A.; Pituco, M.M.; Caixeta, M.P.; Cardona Gallo, S.A.; Botero-Coy, A.M.; Hernández, F.; Torres-Palma, R.A.; Vilar, V.J.P. Ozonation Using a Stainless-Steel Membrane Contactor: Gas-Liquid Mass Transfer and Pharmaceuticals Removal from Secondary-Treated Municipal Wastewater. *Chemosphere* **2024**, *349*, 140888. [[CrossRef](#)] [[PubMed](#)]
38. Piskarev, I.M. The Formation of Ozone-Hydroxyl Mixture in Corona Discharge and Lifetime of Hydroxyl Radicals. *IEEE Trans. Plasma Sci.* **2021**, *49*, 1363–1372. [[CrossRef](#)]
39. Von Sonntag, C.; Dowitz, P.; Xingwang, F.; Mertens, R.; Xianming, P.; Schuchmann, M.N.; Schuchmann, H.-P. The Fate of Peroxyl Radicals in Aqueous Solution. *Water Sci. Technol.* **1997**, *35*, 9–15. [[CrossRef](#)]
40. Tang, L.; Zhou, S.; Li, F.; Sun, L.; Lu, H. Ozone Micronano-Bubble-Enhanced Selective Degradation of Oxytetracycline from Production Wastewater: The Overlooked Singlet Oxygen Oxidation. *Environ. Sci. Technol.* **2023**, *57*, 18550–18562. [[CrossRef](#)]
41. Cao, Y.; Xie, D.; Huang, Y.; Huang, C.; Zhang, K.; Zhang, X.; Wang, S. Investigation of Hydroxyl Radical Yield in an Impact-Jet Hydraulic Cavitator. *Processes* **2022**, *10*, 2194. [[CrossRef](#)]
42. Tesio, A.Y.; Torres, W.; Villalba, M.; Davia, F.; Del Pozo, M.; Córdoba, D.; Williams, F.J.; Calvo, E.J. Role of Superoxide and Singlet Oxygen on the Oxygen Reduction Pathways in Li–O₂ Cathodes at Different Li⁺ Ion Concentration*. *ChemElectroChem* **2022**, *9*, e202201037. [[CrossRef](#)]
43. Tampieri, F.; Ginebra, M.-P.; Canal, C. Quantification of Plasma-Produced Hydroxyl Radicals in Solution and Their Dependence on the pH. *Anal. Chem.* **2021**, *93*, 3666–3670. [[CrossRef](#)] [[PubMed](#)]
44. Lan, W.; Chen, X.; Zhao, Y.; Xie, J. Insights into the Antibacterial Mechanism of Ozone Water Combined with Tea Polyphenols against *Shewanella Putrefaciens*: Membrane Disruption and Oxidative Stress. *Int. J. Food Sci. Technol.* **2022**, *57*, 7423–7433. [[CrossRef](#)]
45. Xu, H.; Yi, L.; Li, C.; Sun, Y.; Hou, L.; Bai, J.; Kong, F.; Han, X.; Lan, Y. Design and Experiment of Ecological Plant Protection UAV Based on Ozonated Water Spraying. *Drones* **2023**, *7*, 291. [[CrossRef](#)]
46. Landa Fernández, I.A.; Monje-Ramirez, I.; Orta Ledesma De Velásquez, M.T. Tomato Crop Improvement Using Ozone Disinfection of Irrigation Water. *Ozone Sci. Eng.* **2019**, *41*, 398–403. [[CrossRef](#)]
47. Szumigaj-Tarnowska, J.; Szafranek, P.; Uliński, Z.; Ślusarski, C. Efficiency of Gaseous Ozone in Disinfection of Mushroom Growing Rooms. *J. Hortic. Res.* **2020**, *28*, 91–100. [[CrossRef](#)]
48. Martínez-Sánchez, A.; Aguayo, E. Effect of Irrigation with Ozonated Water on the Quality of Capsicum Seedlings Grown in the Nursery. *Agric. Water Manag.* **2019**, *221*, 547–555. [[CrossRef](#)]

Disclaimer/Publisher’s Note: The statements, opinions and data contained in all publications are solely those of the individual author(s) and contributor(s) and not of MDPI and/or the editor(s). MDPI and/or the editor(s) disclaim responsibility for any injury to people or property resulting from any ideas, methods, instructions or products referred to in the content.